arXiv:astro-ph/9605142v1 23 May 1996

The Second Measurement of Anisotropy in the Cosmic Microwave Background Radiation at 0°.5 Scales near the Star Mu Pegasi

M. A. Lim[1,3], A. C. Clapp[1,2,4], M. J. Devlin[1,2,5], N. Figueiredo[1,3,7,8], J. O. Gundersen[1,3], S. Hanany[1,2], V. V. Hristov[1,2], A. E. Lange[1,4], P. M. Lubin[1,3], P. R. Meinhold[1,3], P. L. Richards[1,2], J. W. Staren[1,3], G. F. Smoot[1,2,6],and S. T. Tanaka[1,2]

Received _____; accepted _____

Draft August 10, 2008

[1]NSF Center for Particle Astrophysics, Berkeley, CA 94720.

[2]Physics Department, University of California at Berkeley, Berkeley, CA 94720

[3]Physics Department, University of California at Santa Barbara, Santa Barbara, CA 93106

[4]present address: Department of Physics, California Institute of Technology, Pasadena, CA 91125

[5]present address: Department of Physics, Princeton University, Princeton, NJ 08544

[6]Physics Division, Lawrence Berkeley Laboratory, Berkeley, CA 94720

[7] Departamento de Física e Química, Escola Federal de Engenharia de Itajubá, 37500-000 Itajubá, MG, Brazil

[8] Divisão de Astrofísica, Instituto Nacional de Pesquisas Espaciais, 12201-970 São José dos Campos, SP, Brazil

ABSTRACT

During the fifth flight of the Microwave Anisotropy Experiment (MAX5), we revisited a region with significant dust emission near the star Mu Pegasi. A 3.5 cm^{-1} low frequency channel has been added since the previous measurement (Meinhold et al. 1993a). The data in each channel clearly show structure correlated with IRAS 100 μm dust emission. The spectrum of the structure in the 6, 9 and 14 cm^{-1} channels is described by $I_\nu \propto \nu^\beta B_\nu(T_{dust})$, where $\beta = 1.3$ and $T_{dust} = 19$ K and B_ν is the Planck function. However, this model predicts a smaller amplitude in the 3.5 cm^{-1} band than is observed. Considering only linear combinations of the data independent of the best fit foreground spectrum for the three lower channels, we find an upper limit to CMBR fluctuations of $\Delta T/T = \langle \frac{C_l \; l(l+1)}{2\pi} \rangle^{\frac{1}{2}} \leq 1.3 \times 10^{-5}$ at the 95% confidence level. The result is for a flat band power spectrum and does not include a 10% uncertainty in calibration. It is consistent with our previous observation in the region.

Subject headings: cosmic microwave background — cosmology: observations

1. Introduction

Cosmic Microwave Background Radiation (CMBR) anisotropy measurements provide a means of constraining various cosmological models. Several groups have reported measuring CMBR anisotropies at 0.5 to 1° (Cheng et al. 1995, Clapp et al. 1994, de Bernardis et al. 1994, Devlin et al. 1994, Gundersen et al. 1995, Netterfield et al. 1995, Ruhl et al. 1995). However, disentangling the primodial fluctuatations from foreground sources is problematic even if the foreground is understood. The third flight of MAX made an observation in a medium constrast dust region near the star Mu Pegasi and measured anisotropy smaller than seen elsewhere in the same flight (Gundersen et al. 1993, Meinhold et al. 1993a). In order to confirm this measurement, we returned to the Mu Pegasi region with an additional low frequency band centered at 3.5 cm^{-1}.

2. Instrument

MAX is an off-axis Gregorian telescope with a bolometric photometer mounted on an attitude-controlled balloon platform. The instrument has been described extensively elsewhere (Fischer et al. 1992, Alsop et al. 1992, Meinhold et al. 1993b). The telescope has a 1 m off-axis parabolic primary with an elliptical secondary which sinusoidally chops the beam in azimuth at 5.4 Hz with a peak-to-peak throw of 1°.4. The chopped signal is demodulated with a sine-wave lock-in reference. The underfilled optics provide a 0°.5 FWHM beam. An adiabatic demagnetization refrigerator cools the single-pixel, four-band photometer to 85 mK. The four frequency bands are centered at 3.5, 6, 9, and 14 cm^{-1} with respective fractional bandwidths 0.5, 0.5, 0.4, and 0.2. To convert measured antenna temperature differences to 2.726 K thermodynamic temperature differences in each frequency band multiply by 1.62, 2.50, 6.66, and 38.7, respectively.

3. Observation

The instrument was launched from the National Scientific Balloon Facility in Palestine, Texas at 1.16 UT June 20, 1994. We observed CMBR anisotropies in three sky regions near the stars HR5127, Phi Herculis, and Mu Pegasi ($\alpha = 22^{\rm h}49\overset{\rm m}{.}7$, $\delta = 24\overset{\circ}{.}34'$). Tanaka et al. (1996) report on the observations at HR5127 and Phi Herculis. This paper concerns the Mu Pegasi scan.

We observe with a constant velocity scan in azimuth of $\pm 4^\circ$ relative to the pointing star. The left-hand lobe of the antenna pattern was coaligned with the field of view of our CCD cameras and centered on Mu Pegasi. Gyroscope drift was taken out every 400 seconds. The relative offset between the center of the chop and the target star was $0\overset{\circ}{.}55$ in azimuth.

During the Mu Pegasi scan (7.22 UT to 7.76 UT) the gyro malfunctioned and moved the chop center with a trajectory tilted 10±1.5 degrees from horizontal. The orientation of the gondola was still vertical. We verified the orientation and trajectory with the positions of stars in the CCD camera field of view. We did not observe in the same orientation as in MAX3 and we do not expect the morphology to be identical. The other MAX 5 observations displayed no significant tilt.

We calibrated the instrument before and after the observation using a membrane transfer standard (Fischer et al. 1992). We observed Jupiter from 4.86 UT to 4.95 UT to measure the beam size and position and to confirm the membrane calibration. Using the best-fit beam size and the membrane calibration, the derived temperature of Jupiter agrees with Griffin et al. (1986) to within 10%. We assume a 10% uncertainty in calibration. The calibration is such that a chopped beam centered between sky regions with temperatures T_1 and T_2 would yield $\Delta T = T_1 - T_2$ in the absence of instrumental noise.

Anisotropy experiments are potentially susceptible to off-axis response to local sources,

particularly the Earth, the balloon, and the moon. The unchopped off-axis response in the 3.5 cm^{-1} band is $\geq$ 70 dB below the on-axis response from 15° to 25° in elevation under the boresight. We have not made comparable measurements of the chopped sidelobe response in azimuth. Mu Pegasi was $\sim$ 137° away from the Moon during the observation.

4. Data Analysis

4.1. Data Reduction

We remove transients due to cosmic rays using an algorithm described by Alsop et al. 1992. This procedure excludes approximately 18% of the data. We demodulate the detector output using the sinusoidal reference from the chopping secondary to produce antenna temperature differences ΔT_A on the sky. This produces a data set in phase and a data set 90° out of phase with the optical signal. The noise averaged over the observation gives respective CMBR sensitivities of 440, 240, 610, and 5100 $\mu K\sqrt{s}$ in the 3.5, 6, 9, and 14 cm^{-1} bands.

The averages of the measured instrumental offsets in antenna temperature were 0.6, 0.15, 1.4, and 2.8 mK in the 3.5, 6, 9, and 14 cm^{-1} bands. We attribute this to chopped emissivity differences on the primary mirror and chopped atmospheric emission. The offset drifts in the higher frequency bands with amplitudes of 0.7 mK and 1.0 mK in the 9 and 14 cm^{-1} bands over a time scale of 3 minutes. Comparison of the first and second halves of the scan shows that the signal is stable in the 3.5, 6, and 9 cm^{-1} bands, but not so in the 14 cm^{-1} band. The instability in the 14 cm^{-1} band could be caused by sidelobe pickup or atmosphere. To increase the stability, we subtract an offset and gradient, as in a ground based observation, with a linear least squares fit to each pass going from -4° to +4° or +4° to -4°. Each half scan takes 72 s.

For each observation we calculated the means and 1 σ uncertainty of the antenna temperature differences for 29 pixels separated by $17'$ on the sky. Figure 1 shows the antenna temperature differences as a function of scan angle for the Mu Pegasi scan. There is significant structure ($\chi^2 = 38$, 86, 86, 79 for 27 DOF) that is well correlated ($R \gtrsim 0.5$) in all channels of the in-phase data.

4.2. Foregrounds

Possible astrophysical sources for the signal in the Mu Pegasi scan are free-free or synchrotron radiation, interstellar dust (ISD) emission, radio point sources, or CMBR. From the rising spectrum in ΔT_A in Figure 1 it is clear that CMBR, free-free or synchrotron radiation alone is not responsible for the signal. The latter two cases are also excluded by amplitude and morphology arguments. If we extrapolate the Haslam 408 MHz map (Haslam, C.G.T. et al.) to our frequencies using $\Delta T_A \propto \nu^{-2.1}$ for free-free emission and $\Delta T_A \propto \nu^{-2.7}$ for synchrotron radiation and convolve with our chopped beam pattern, we find that the former produces $< 10\%$ of the signal in the 3.5 cm^{-1} channel and the latter $< 1\%$. Furthermore, the morphology does not match that of the data. An automated point source search [1] has yielded no candidates within $90'$ that could produce a signal greater than 10 μK.

Previous experience in this region leads us to expect ISD to be the main contributor to our high frequency signal. We convolved the IRAS 100 μm maps with our chopped beam pattern and produced simulated scans. We found the scale factors that minimized the

[1] The NASA/IPAC Extragalactic Database (NED) is operated by the Jet Propulsion Laboratory, California Institute of Technology, under contract with the National Aeronautics and Space Administration

reduced χ^2 from 100 μm simulations to each data channel separately and then normalized them to the 3.5 cm^{-1} band. The results are shown in Table 1. The best fit morphology and spectrum are superimposed over the data in Figure 1. If we consider the 6, 9, and 14 cm^{-1} bands only, these scale factors indicate a warm dust spectrum $I_\nu \propto \nu^\beta B_\nu(T_{dust})$, where $\beta = 1.3^{+0.2}_{-0.1}$ and $T_{dust} = 19^{+1}_{-1}$ K. This is consistent with our previous results (Meinhold et al. 1993a, Fischer et al. 1995). However, the rise in amplitude in the 3.5 cm^{-1} band is not well explained by a warm dust or warm and cold dust model.

There are two possible causes for the rise in amplitude in the lowest band. One is a high frequency leak in the filters. Pre-flight systematic tests with a thick grill high pass filter showed that high frequency leakage above 20 cm^{-1} was less than 0.8% of the total band response to a 300K blackbody chopped relative to a 77K blackbody. Using measured filter transmittances and the amplitude of dust fluctuations in this sky region (Fischer et al. 1995), we calculated that maximum modeled high frequency leakage of power from dust fluctuations contributes less than ∼1% of the expected inband power from CMB fluctuations and less than 2% of the observed structure. Another candidate is a correlated low frequency component [2]. However, fits of two component models did not conclusively distinguish between the possibilities, such as CMBR + ISD and HII + ISD.

We conclude the following about the foreground contaminant: The correlation between the 14 cm^{-1} band and the other bands indicates a single foreground morphology. Whatever the nature of the foreground, the relative amplitudes in the bands are given in Table 1 column 2. Because of the excellent fit of the IRAS 100 μm maps to the 14 cm^{-1} channel, we assume that the ISD dominates over any other possible high frequency contaminant.

---

[2]Kogut et al. report correlation between HII and ISD at angular scales $> 7°$. However, our cross-correlation coefficient 3.5 cm^{-1}/IRAS 100 μmis30$\pm$6 mK(MJy/sr)$^{-1}$ which should be compared to 4.56 ± 3.89 mK(MJy/sr)$^{-1}$ for DMR 90 GHz/DIRBE 100 μm

5. Discussion

We analyze the three channels most sensitive to CMBR, 3.5, 6 and 9 cm^{-1} for anisotropy in the presence of a single foreground morphology with the spectrum found above. We use maximum likelihood methods assuming uniform prior to set limits of the rms temperature fluctuation in the data, $Q \equiv Q_{rms-PS} \equiv \langle Q_{rms} \rangle^{0.5}$ (Smoot et al. 1992, Wright, E. et al. 1994). The likelihood, L, is given by

$$L \propto \frac{\exp(-\frac{1}{2}\mathbf{T}^T\mathbf{M}^{-1}\mathbf{T})}{\sqrt{\det(\mathbf{M})}} \tag{1}$$

where $\mathbf{T}$ is the data vector of all 29 bins and 3 channels and $\mathbf{M}$ is the full covariance matrix for a flat band power spectrum.

We marginalize the data to account for the best fit foreground spectrum given in Table 1 and the offset and gradient removal (Dodelson & Stebbins 1994, Bunn et al. 1994, Bond et al. 1991). To do so, we construct a data vector and covariance matrix, $\mathbf{T}^{ind} = \mathbf{z}^T\mathbf{R}^T\mathbf{T}$ and $\mathbf{M}^{ind} = \mathbf{z}^T\mathbf{R}^T\mathbf{M}\mathbf{R}\mathbf{z}$, where $\mathbf{z}$ and $\mathbf{R}$ account for both a single foreground spectrum and offset and gradient removal respectively. Using $\mathbf{M}^{ind}$ and $\mathbf{T}^{ind}$ in equation (1) yields an upper limit, $Q < 23$ μK (95% confidence level) or $\Delta T/T \ < \ 1.3 \times 10^{-5}$.

When MAX3 Mu Pegasi is analyzed in a fashion similar to this paper, we find $Q < 28$ μK (95% confidence level) when marginalized for the dust model in Meinhold et al. 1993a. The two data sets are consistent with each other for similar analysis techniques. Furthermore, the MAX5 Mu Pegasi upper limit is consistent with the result from HR5127 ($\Delta T/T = 1.2^{+0.4}_{-0.3} \times 10^{-5}$) although roughly so with Phi Herculis ($\Delta T/T = 1.9^{+0.7}_{-0.4} \times 10^{-5}$) which were also observed in that flight.

6. Conclusion

We have presented new results from a search for CMBR anisotropy with high sensitivity at $0\overset{\circ}{.}5$ angular scales near the star Mu Pegasi. Free-free and synchrotron radiation are excluded as the main source of signal on amplitude and spectral arguments. There are no strong point sources in the field. The morphology of the observed structure is consistent with known interstellar dust but not the spectrum. The structure in the 6, 9 and 14 cm^{-1} channels is fit by a single dust model power law $I_\nu \propto \nu^\beta B_\nu(T_{dust})$, where $\beta = 1.3$, and $T_{dust} = 19$ K. We cannot rule out the possibility that the structure is a correlated combination of dust and CMBR or dust and free-free radiation. Linear combinations of the data independent of the best fit spectrum yield a $\Delta T/T \ < \ 1.3 \times 10^{-5}$. (95% confidence level) The results are consistent with our previous observation in the region. These data are available from the authors.

This work was supported by the National Science Foundation through the Center for Particle Astrophysics (cooperative agreement AST 91-20005), the National Aeronautics and Space Administration under grants NAGW-1062 and FD-NAGW-1221, the University of California, and previously the California Space Institute. We would like to thank O. Levy for his assistance with the flight preparation and the MSAM team for borrowed equipment during the flight campaign. The IRAS map used in the analysis was created by Skyview, maintained by Goddard Space Flight Center. N.F. was partially supported by Conselho Nacional de Desenvolvimento Científico e Tecnológico, Brazil.

Table 1. Scale factors for fit to IRAS 100 μm dust morphology

Frequency (cm^{-1})	$\frac{\Delta T_A^i}{\Delta T_A^{3.5}}$ [a]	Reduced χ^2
3.5	1.00	26/27
6	0.55	56/27
9	0.74	43/27
14	1.00	28.5/27

[a] These are the ratios of the differential antenna temperatures for the best fit spectrum

REFERENCES

Alsop, D. C., et al. 1992, ApJ, 395,317

Bond, J.R., Efstanthiou,G., Lubin,P.M., Meinhold, P.R. 1991, Phys. Rev. Lett., 66, 2179

Bunn, E., et al., 1994, ApJ, 429,1

Cheng, E. S., et al. 1995, ApJ, submitted, preprint `astro-ph/9508087`

Clapp, A. C., et al. 1994, ApJ, 433, L57

de Bernardis, P. et al. 1994, ApJ, 422, L33.

Devlin, M. J., et al. 1994, ApJ, 430, L1

Dodelson, S. & Stebbins, A. 1994, ApJ, 433, 440

Fischer, M. L., et al. 1992, ApJ, 388, 242

Fischer, M. L., et al. 1995, ApJ, 444, 226

Griffin, M. J., et al. 1986, Icarus, 65, 244

Gundersen, J. O., et al. 1993, ApJ, 413, L1

Gundersen, J. O., et al. 1995, ApJ, 443, L57

Haslam, C.G.T. et al. 1982, A&AS,47,1

Kogut, A., et al. 1995, astro-ph/9509151

Meinhold, P. R., et al. 1993a, ApJ, 409, L1

Meinhold, P. R., et al. 1993b, ApJ, 406, 12

Netterfield, C. B., Jarosik, N., Page, L., Wilkinson, D., & Wollack, E. 1995, ApJ, 445, L69.

Ruhl, J. E., Dragovan, M., Platt, S. R., Kovac, J., & Novak, G. 1995, ApJ, 435, L1.

Smoot, G.F., et al. ApJ,396,L1 (1992)

Tanaka, S. et al. submitted ApJ

Wheelock, S. L. et al. 1994, *IRAS Sky Survey Atlas Explanatory Supplement*, JPL Publication 94-11. JPL, Pasadena.

Wright, E., et al. ApJ, 420, 1 (1994)

This manuscript was prepared with the AAS LaTeX macros v4.0.

Fig. 1.— Antenna temperature differences plotted as a function of scan angle. Superimposed over the data are IRAS 100 μm dust morphologies scaled for different spectra. The dashed line is for a spectrum with $\beta = 1.3$ and $T_{dust} = 19\ K$. The solid line is for a similar morphology but with the amplitudes chosen to minimize χ^2.

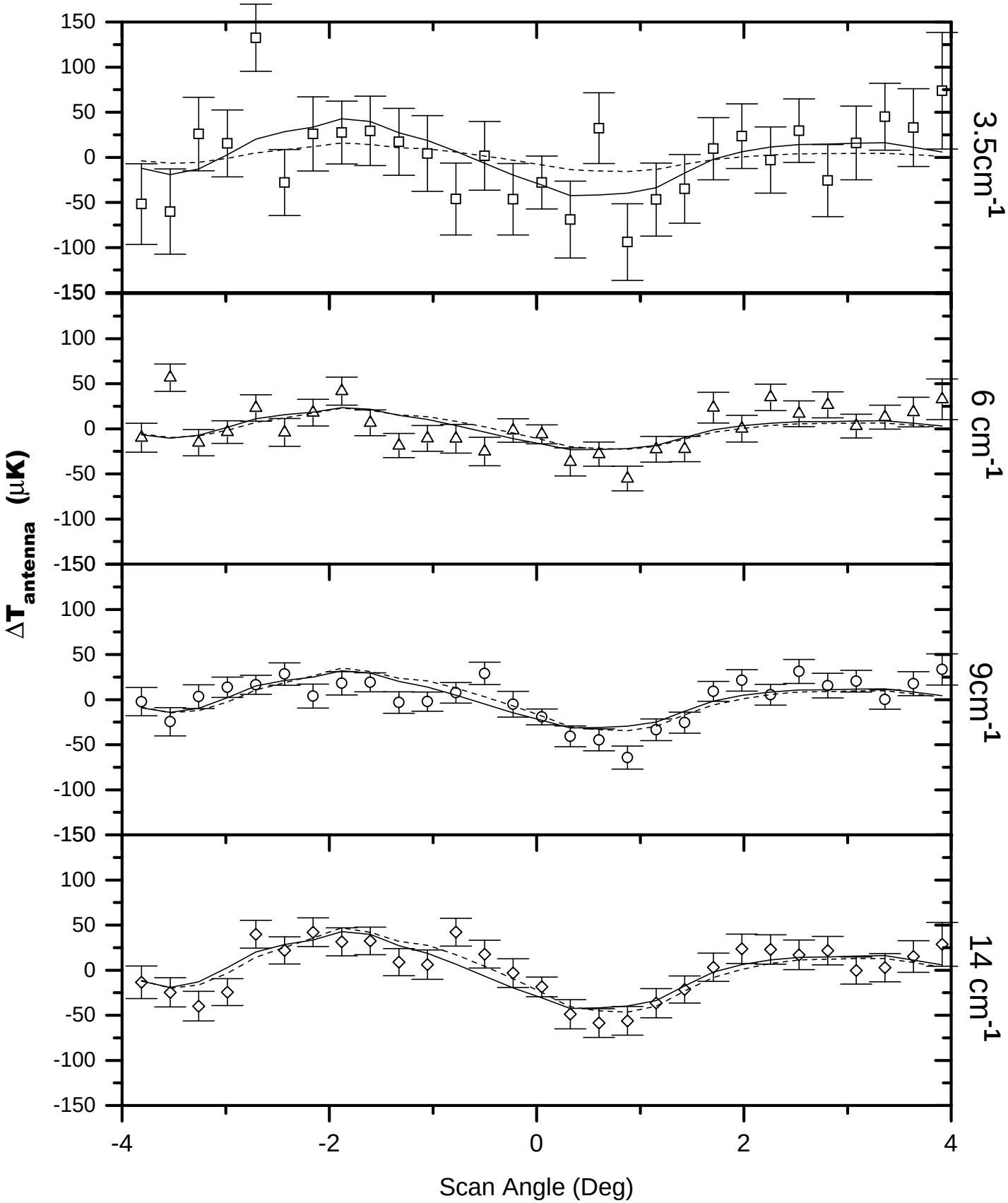
150
100
50
0
-50
-100
-150
3.5cm-1
6 cm-1
9cm-1
14 cm-1
ΔTantenna (μK)
-4
-2
0
2
4
Scan Angle (Deg)